The role of glacial gravel in community development of vascular plants on the glacier forelands of the Third Pole

WEI Tianfeng[1], SHANGGUAN Donghui[2,3,4*], TANG Xianglong[1*], QIN Yu[2]

[1] School of Architecture and Urban Planning, Lanzhou Jiaotong University, Lanzhou 730070, China;
[2] State Key Laboratory of Cryospheric Sciences, Northwest Institute of Eco-Environment and Resources, Chinese Academy of Sciences, Lanzhou 730000, China;
[3] University of Chinese Academy of Sciences, Beijing 100049, China;
[4] China-Pakistan Joint Research Center on Earth Sciences, Chinese Academy of Sciences and Higher Education Commission Pakistan, Islamabad 45320, Pakistan

Abstract: On a deglaciated terrain, glacial gravel is the primary component of the natural habitat for vascular plant colonization and succession. Knowledge regarding the role of glacial gravel in vascular plant growth, however, remains limited. In this study, an unmanned aerial vehicle (UAV) was used to investigate plant family composition, species richness, fractional vegetation cover (FVC), and gravel cover (GC) along elevational gradients on the three glacier forelands (Kekesayi, Jiangmanjiaer, and Koxkar Baxi) of the Third Pole (including the eastern Pamir Plateau and western Tianshan Mountains) in China. We then analyzed the spatial characteristics of vascular plants followed by exploring the effect of glacial gravel on vascular plants. Findings indicated that FVC on these glacier forelands generally decreased as the elevation increased or distance from the current glacier terminus decreased. The shady slope (Kekesayi) was more vegetated in comparison to the sunny slope (Jiangmanjiaer) at the glacier basin scale, and the warm and humid deglaciated terrain (Koxkar Baxi) had the highest FVC at the regional scale. Plant family composition and species richness on the glacier forelands decreased with rising elevation, with the exception of those on the Jiangmanjiaer glacier foreland. The relationships between FVC and GC presented negative correlations; particularly, they exhibited variations in power functions on the Kekesayi and Jiangmanjiaer glacier forelands of the eastern Pamir Plateau and a linear function on the Koxkar Baxi glacier foreland of the western Tianshan Mountains. Glacial gravel was found to be conducive to vegetation colonization and development in the early succession stage up until vascular plants adapted to the cold and arid climatic condition, whereas it is unfavorable to the expansion of vascular plants in the later succession stage. These findings suggested that the spatial difference of plant characteristics had close connections with regional climatic and topographic conditions, as well as glacial gravel distribution. In addition, we concluded that aerial photographs can be an asset for studying the functions of micro-environment in vegetation colonization as well as succession on the glacier forelands.

Keywords: vascular plants; fractional vegetation cover; glacial gravel; glacier foreland; unmanned aerial vehicle; Pamir Plateau; Tianshan Mountains

Citation: WEI Tianfeng, SHANGGUAN Donghui, TANG Xianglong, QIN Yu. 2022. The role of glacial gravel in community development of vascular plants on the glacier forelands of the Third Pole. Journal of Arid Land, 14(9): 1022–1037. https://doi.org/10.1007/s40333-022-0073-1

*Corresponding authors: SHANGGUAN Donghui (E-mail: dhguan@lzb.ac.cn); TANG Xianglong (E-mail: tangxl@mail.lzjtu.cn)
Received 2022-05-07; revised 2022-08-05; accepted 2022-08-07

1 Introduction

There are a large number of mountain glaciers in China. According to the second Chinese Glacier Inventory (CGI) (Liu et al., 2015) and Randolph Glacier Inventory (RGI) 6.0 (RGI Consortium, 2017), the country's glaciers cover 5.18×10^4 km^2 or 7.3% of the world's total glacial area. This is the highest percentage with the exception of the Arctic and Antarctic (70.58×10^4 km^2). Due to global warming, glaciers worldwide have typically been retreating since the end of the Little Ice Age (approximately 1850) (Leclercq et al., 2011; IPCC, 2012), and China is no exception (Li et al., 1998; Liu et al., 2003; Shangguan et al., 2006; Zhang et al., 2016; Li et al., 2019). Uncovered surfaces after glacier retreat offer excellent opportunities to examine the processes of primary vegetation succession in the field. As a result, a number of research findings on succession dynamics along with factors impacting vegetation development have been published, which are primarily implemented in High Arctic, European mountainous areas, and North America (Raffl et al., 2006; He and Tang, 2008; Burga et al., 2010; Wietrzyk et al., 2018; Wei et al., 2021). In China, the prime focus of the studies on the spatial distribution and succession of vegetation is on several glacier forelands, which consist of Yulong Snow Mountain, Tianshan Mountains, and Gongga Mountain (Li and Xiong, 1995; Chang et al., 2014; Wei et al., 2021). These works have provided valuable vegetation information on the glacier forelands of the Third Pole region in China. However, in comparison to those in the aforementioned regions, there is a scarcity of related studies in this field (Third Pole region).

All stages of plant community development on the glacier forelands are dominated by both biotic and abiotic factors, whereas in the early stage of vegetation succession, abiotic control plays a more crucial role (Houle, 1997; Jumpponen et al., 1999). Glacial gravel, which comes either supraglacially from nunataks and valley sides or from erosion of the subglacial bed (Boulton, 1978), is quite prevalent on the glacier forelands. Scientists have taken a keen interest in it since vegetation tends to grow in surrounding glacial gravel. According to the previous publications (Rooney, 1997; Mong and Vetaas, 2006), glacial gravel plays a controversial role in vegetation colonization as well as the development of the glacier forelands. In particular, some studies have pointed out that glacial gravel on the glacier forelands prevents disturbances from herbivores (Rooney, 1997) and provides relatively safe sites for the early colonization of several pioneer plants (Stöcklin and Bäumler, 1996; Jumpponen et al., 1999; Niederfriniger Schlag and Erschbamer, 2000). While on the other hand, other studies have argued that the potentially protective glacial gravel at a microsite becomes an obstacle for seedling establishment because the available space for germination is occupied (Mong and Vetaas, 2006). Therefore, there is an urgent need to further explore the spatial changes of vegetation characteristics as well as the impact of glacial gravel on vegetation colonization and development. In order to comprehensively understand this scientific question, our investigation had to be expanded to several glacier forelands with various regional typographic and climatic conditions.

Glacier forelands are characterized by complex terrains, unique ecosystems, and harsh environments, making the field investigation of vegetation dynamics more challenging. Up to now, traditional ground sampling has been a valuable approach and has been extensively applied in field surveys (Niederfriniger Schlag and Erschbamer, 2000; Mong and Vetaas, 2006; Raffl et al., 2006; Burga et al., 2010; Wietrzyk et al., 2018), but this methodology is time-consuming and labor-intensive, and requires trampling fragile habitats (Lee and Yeh, 2009; Martínez-López et al., 2014). Additionally, the free satellite image is difficult to utilize for the assessment of vegetation characteristics on the glacier forelands owing to its low resolution. In contrast, the unmanned aerial vehicle (UAV) provides an ideal solution to this problem due to its natural advantages, such as increased field efficiency, effective avoidance of human disturbance, the automatic acquisition of high-resolution images at the quadrat scale, and the ability to repeatedly observe the same area after setting the flight line (Sun et al., 2018). Furthermore, the UAV can easily acquire vegetation data in inaccessible areas. These advantages make the UAV technique suitable for vegetation monitoring in a variety of topographic conditions including glacier forelands.

Fractional vegetation cover (FVC), plant family composition, species richness, dominant species, and gravel cover (GC; the ratio of the vertical projected area of glacial gravel to the total ground area) along chronosequences were investigated by integrating ground-based sampling and aerial photography on the three glacier forelands of China's eastern Pamir Plateau and western Tianshan Mountains in this study. Following that, we analyzed the variation characteristics of these vegetation indices during primary succession along with the relationship between GC and FVC. This study aims to characterize the spatial variations of vegetation characteristics (FVC, plant family composition, and species richness), examine the spatial heterogeneity of vegetation under various regional typographic and climatic conditions, and assess the influence of glacial gravel on vegetation community development. The findings of this study will assist investigators of primary vegetation succession and biodiversity, and aid in regional ecological conservation and sustainability in the Third Pole region.

2 Materials and methods

2.1 Study area

The study area is situated in the Third Pole region and spans across the eastern Pamir Plateau and western Tianshan Mountains in Xinjiang Uygur Autonomous Region, China. A total of three glacier forelands namely Kekesayi, Jiangmanjiaer, and Koxkar Baxi were surveyed. Within each glacier foreland, the sampling sites were established along elevational gradients (Fig. 1). The sites in the eastern Pamir Plateau were distributed in the retreat areas of modern and paleo glaciers (elevation ranges of 3843–4004 m a.s.l. for the Kekesayi glacier and 3631–4241 m a.s.l. for the Jiangmanjiaer glacier), whereas those in the western Tianshan Mountains were primarily chosen in the deglaciated terrain of the modern glacier (elevation range of 2979–3099 m a.s.l. for the Koxkar Baxi glacier).

The Kekesayi glacier (code number of 5Y663D0087 from the Chinese Glacier Inventory) and Jiangmanjiaer glacier (code number of 5Y663D0004 from the Chinese Glacier Inventory), which are typical valley glaciers, are situated in the same glacier basin (Fig. 1b–d) under the ice caps of the Muztagata Peak and Kongur Peak, respectively. With an approximate length of 18.0 km and an extent of 86.50 km^2, the debris-covered Kekesayi glacier extends from the east to the north and is by far the largest glacier of the Muztagata Peak (Shangguan et al., 2006; Seong et al., 2009a, b). The Jiangmanjiaer glacier, which is 14.8 km long and extends over 45.08 km^2, is the longest glacier on the southwestern slope of the Kongur Peak (Wang et al., 2011). The field investigation of the moraine ridge and previous publications on the quaternary glacier landform revealed that the entire Muztagata Peak and Kongur Peak were covered by huge glaciers in the historical period, and glaciers even extended into the Kara Kol Lake during the glacial maximum of these areas (Cui, 1960). However, based on remote sensing data, their frontal positions have had almost no visual changes in the last four decades (Holzer et al., 2015). The Muztagata Peak and Kongur Peak are mainly controlled by the upper-level westerly circulation and local circulation, and moisture transference is difficult here because of the "blocking effect" of surrounding high mountains (Yu et al., 2006). As a result, the two peaks exhibit a cold and semi-arid continental climate. The Taxkorgan meteorological station, situated approximately 50.0 km south of the Muztagata Peak, is the sole station above 3000 m a.s.l. on the eastern Pamir Plateau. From 1957 to 2010, the mean annual temperature at this station was measured as 3.4°C, the mean summer temperature as 15.1°C (June–August), and the mean annual precipitation as 70.2 mm (Yan et al., 2013; Yang et al., 2014). The distribution of vegetation types along elevational gradients is as follows: meadow (below 3500 m a.s.l.), desert vegetation (3500–4000 m a.s.l.), alpine grassland vegetation (above 4000 m a.s.l.), and alpine sparse vegetation (above 4500 m a.s.l.); the floristic composition consists of *Ceratoides*, *Graminoids*, *Artemisia*, *Stipa*, etc. (Wang et al., 2016). The vegetation characteristics of the two glacier forelands, nevertheless, were obviously different (Fig. 2a–f).

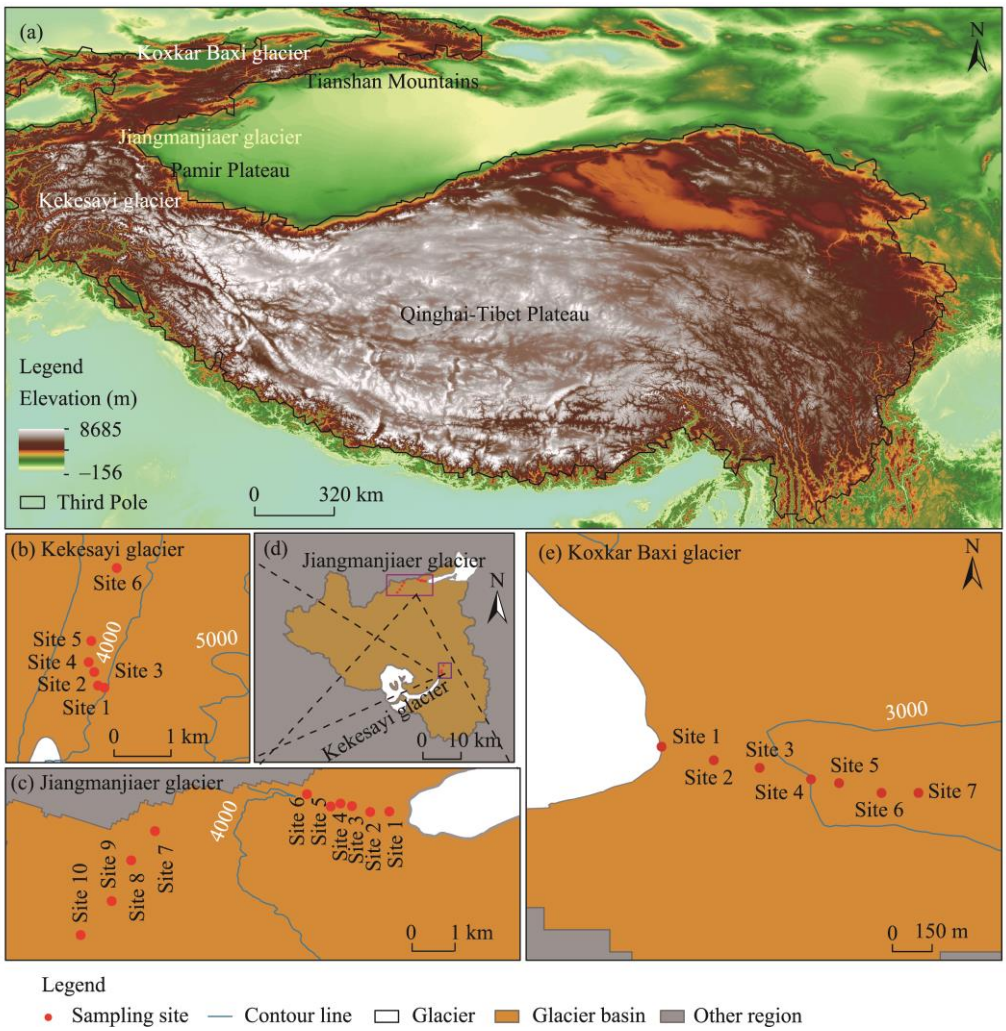

Fig. 1 Overview of the study area (a) and distribution of sampling sites in the Kekesayi glacier (b) and Jiangmanjiaer glacier (c) of the eastern Pamir Plateau (d) and in the Koxkar Baxi glacier of the western Tianshan Mountains (e)

The Koxkar Baxi glacier (code number of 5Y674A0005 from the Chinese Glacier Inventory), situated on the southern slope of the Tuomuer-Khan Tengri Mountain in the western Tianshan Mountains (Fig. 1), is a typical continental glacier with the length of about 26.0 km, an area of 83.60 km^2, and elevations of 3020–6342 m a.s.l. (Zhang et al., 2007). It is a glacier covered in debris, and since the 1980s, its terminus has been retreating at an average rate of 0.5–1.5 m/a (Xie et al., 2007). The mid-latitude westerlies that originate from the Atlantic Ocean have the most impact on the region. The Koxkar Baxi glacier presents a sub-humid climate with the mean annual precipitation of 669.4 mm at 3000 m a.s.l. (Li et al., 2012). The mean summer temperature (June–August) is as high as 11.0°C at 3007 m a.s.l. (Han et al., 2008). The following vegetation types can be found around the glacier: alpine meadow (2900–3600 m a.s.l.) and alpine cushion plants (3600–4250 m a.s.l.) (Sabit et al., 2016). The land near the glacier terminus is barren and covered by massive glacial gravel, but an alpine meadow occurs at 2979 m a.s.l. (Fig. 2g–i).

2.2 Unmanned aerial vehicle (UAV) survey and data collection

The Mavic Pro (Fig. 3), which was employed in this study, is an electric rotary quadcopter manufactured by DJI Innovation Company, Shenzhen City, China. It is equipped with a high-precision vision positioning system that enables it to precisely capture images with geodetic

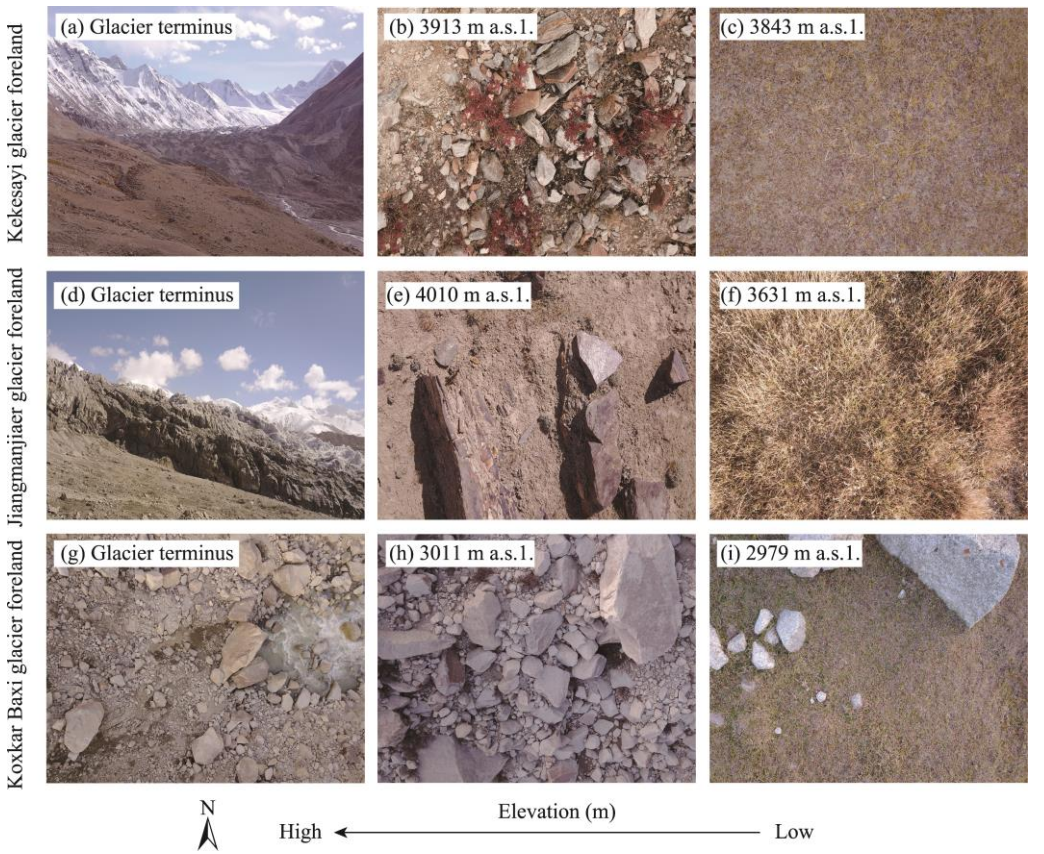

Fig. 2 Photographs of surface features on the Kekesayi glacier foreland (a, b, and c), Jiangmanjiaer glacier foreland (d, e, and f), and Koxkar Baxi glacier foreland (g, h, and i) along elevational gradients

accuracy even in conditions having a poor global navigation satellite system signal. A three-band FC220 digital camera, integrated in the front of Mavic Pro, features a 12-megapixel resolution (4000×3000 pixels) and maintains a horizontal orientation when stationary.

During the period from 26 September to 2 October, 2018, we selected 23 sampling sites along elevational gradients on the basis of the vegetation characteristics (FVC, plant height, and vegetation type) on the three glacier forelands. These sites had obvious differences in the plant community characteristics and could reflect the real-life feasibility of vegetation distribution. At each site, the UAV was taken from 2.0 m in height and covered the quadrats with 40 m×40 m in size (Fig. 3). Prior to each flight, waypoints were adjusted to follow the topography of the glacier forelands. The UAV took photographs vertically downward while flying autonomously between waypoints generated in the flight planning software. During the flight, the camera was triggered every 3 s as the UAV traveled at 3.0 m/s, and all images were stored in the JPEG format to aid later processing. The white balance of the camera was set in accordance with the actual weather conditions. At least 16 images were obtained on each flight under normal circumstances. The high spatial resolution (0.07 cm) of all images was beneficial for extracting the necessary underlying surface information.

No meteorological station existed on the three glacier forelands, with the exception of one automatic weather station on the Koxkar Baxi glacier foreland. Hence, meteorological data (temperature and precipitation) were calculated through empirical formulas. On the Kekesayi and Jiangmanjiaer glacier forelands, the following equations were applied:

$$AP_{Pamir} = 605.0 + 13.7 \times \frac{A_i - 7010}{100}, \quad (1)$$

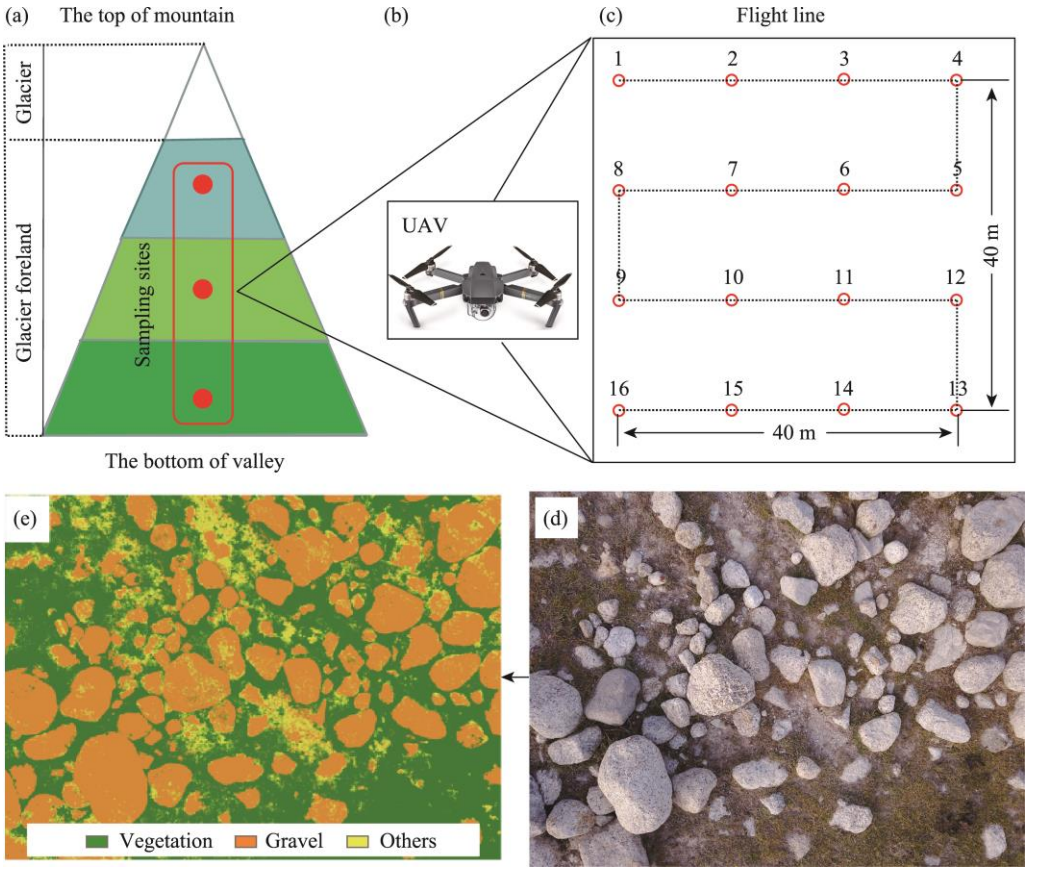

Fig. 3 Field experimental design of the sampling site selection and unmanned aerial vehicle (UAV) survey, as well as the later processing of aerial photographs. (a), distribution of sampling sites along elevational gradients; (b), photograph showing the UAV; (c), design of UAV survey; (d), aerial photograph; (e), interpretation of aerial photograph.

$$\mathrm{AMT_{Parmir}} = 0.70 - 0.71 \times \frac{A_i - 3250}{100}, \tag{2}$$

where $\mathrm{AP_{Pamir}}$ and $\mathrm{AMT_{Pamir}}$ denote the annual precipitation (mm) and annual mean temperature (°C) of the eastern Pamir Plateau, respectively; values of 13.7 and 605.0 are the precipitation lapse rate (mm/100 m) and annual precipitation (mm) at 7010 m a.s.l., respectively (Duan et al., 2007); values of 0.71 and 0.70 are the temperature lapse rate (°C/100 m) and annual mean temperature (°C) at 3250 m a.s.l., respectively (Luo, 1994; He et al., 2005); and A_i represents the elevation variable (m a.s.l.).

On the Koxkar Baxi glacier foreland, the equations used are as follows:

$$\mathrm{AP_{Tianshan}} = 669.4 + 49.8 \times \frac{A_i - 3000}{100}, \tag{3}$$

$$\mathrm{AMT_{Tianshan}} = 0.70 - 0.63 \times \frac{A_i - 2950}{100}, \tag{4}$$

where $\mathrm{AP_{Tianshan}}$ and $\mathrm{AMT_{Tianshan}}$ reflect the annual precipitation (mm) and annual mean temperature (°C) of the western Tianshan Mountains, respectively; values of 49.8 and 669.4 are the precipitation lapse rate (mm/100 m) and annual precipitation (mm) at 3000 m a.s.l., respectively (Li et al., 2012); and values of 0.63 and 0.70 are the temperature lapse rate (°C/100 m) and annual mean temperature (°C) at 2950 m a.s.l., respectively (measured data) (Han et al., 2008).

The calculated results are presented in Table 1.

Table 1 Annual mean temperature (AMT) and annual precipitation (AP) on the three glacier forelands

Glacier foreland	Elevation (m a.s.l.)	AMT (°C)	AP (mm)	Aspect
Kekesayi glacier foreland	3843–4004	–4.7 to –3.5	171.1–193.2	Northeast
Jiangmanjiaer glacier foreland	3631–4241	–6.3 to –2.0	142.1–225.6	Southwest
Koxkar Baxi glacier foreland	2979–3099	–0.2 to 0.5	658.9–718.7	South

2.3 Evaluation of fractional vegetation cover (FVC) and gravel cover (GC)

For the purpose of accurately obtaining ground-cover data such as FVC and GC, we removed low-quality images and adopted the traditional maximum likelihood classifier to process high-quality ones by utilizing the ENVI software (Harris Geospatial Solutions, Boulder, CO, USA). The aerial photographs were positioned by Pix4D software (Pix4D Company, Lausanne, Switzerland) prior to classification. The deformation of the images was negligible due to low flight height (2.0 m) and relatively flat aerial sites. Individual photographs were classified independently using a supervised classification-based maximum likelihood classification method. According to the purpose of this study, we divided photographs into three land cover types, which are vegetation, glacial gravel, and others (such as water body, barren land, and so on) (Fig. 3). We conducted the classification accuracy assessments of the resulting layers of aerial photographs by contrasting the sample class of the classified layer with the reference layer. The overall accuracy and Kappa coefficient were computed so as to evaluate the degree of the classification accuracy of the error matrix (Muzein, 2006). The overall accuracy is the sum of correctly classified values (diagonals) divided by the total number of randomly generated reference values of the error matrix (Lillesand and Kiefer, 2000). The Kappa coefficient, which determines the difference between the actual agreement of classified map and the chance agreement of random classifier compared with reference data, was calculated as follows:

$$K_{hat} = \frac{N\sum_{i=1}^{k} x_{ab} - \sum_{i=1}^{k}\left(x_a \times x_b\right)}{N^2 - \sum_{i=1}^{k}\left(x_a \times x_b\right)}, \tag{5}$$

where K_{hat} is the Kappa coefficient; N presents the total number of values; $\sum_{i=1}^{k} x_{ab}$ is the observed accuracy; and $\sum_{i=1}^{k}\left(x_a \times x_b\right)$ is the chance accuracy.

The results were tested with a Kappa coefficient of over 0.58, which indicated that data quality was acceptable. Finally, we calculated FVC and GC based on the classified results, and the equations are as follows:

$$\text{FVC}\ (\%) = \frac{\text{Pixcel number}_v}{\text{Pixcel number}_t} \times 100\%, \tag{6}$$

$$\text{GC}\ (\%) = \frac{\text{Pixcel number}_g}{\text{Pixcel number}_t} \times 100\%, \tag{7}$$

where FVC is the fractional vegetation cover (%); GC is the gravel cover (%); Pixel number$_v$ is the pixel number of vegetation; Pixel number$_g$ is the pixel number of glacial gravel; and Pixel number$_t$ is the total pixel number within each aerial image.

In this study, we regarded the mean FVC and mean GC calculated by 16 aerial photographs as reference data at each site. The flowchart for the calculation of FVC and GC is shown in Figure 4.

2.4 Calculations of plant family composition, dominant species, and species richness

The plant families were identified by aerial photographs (see Wei et al. (2021) for details), and the identified results were tested by the ground-based sampling. A total of 12 vascular plant families were identified in this study (Table 2). Besides, the dominant species within each sampling site were confirmed by the occurrence frequency as well as the cover of each species in 16 aerial photographs. This indicated that the dominant species had the highest occurrence frequency and coverage. Species richness is a common vegetation index that reflects species diversity in a

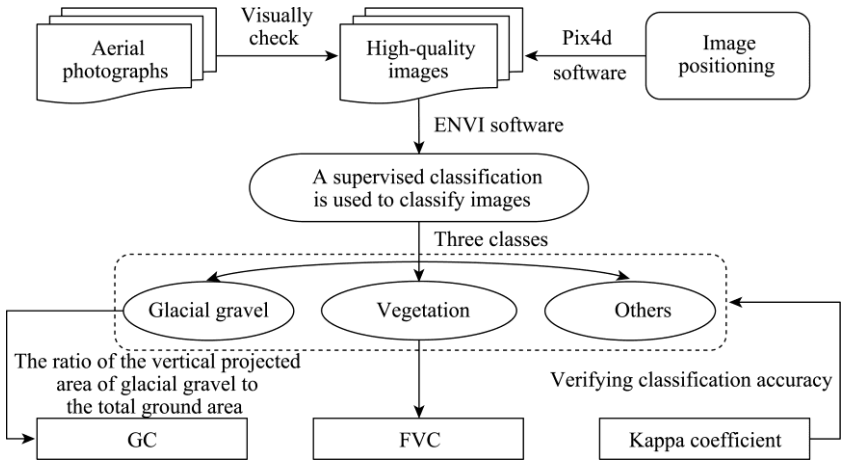

Fig. 4 Flowchart for the calculation of fractional vegetation cover (FVC) and gravel cover (GC)

community or biotope (Karen et al., 2004). In this study, based on the characteristic difference of a variety of species, we visually identified and counted the species number by the 16 images within each site. After that, the species richness was obtained using the equation below:

$$D = \text{Species number appeared in unit area}, \tag{8}$$

where D refers to the total number of species at each sampling site, namely, the species number appearing in 16 aerial photographs.

Table 2 Plant family composition at sampling sites of the three glacier forelands

Glacier foreland	Elevation (m a.s.l.)	Plant family composition
Kekesayi glacier foreland	4004	Cyperaceae and Compositae
	3963	Cyperaceae, Compositae, and Gramineae
	3913	Cyperaceae, Compositae, Gramineae, and Rosaceae
	3890	Cyperaceae, Compositae, Gramineae, Rosaceae, Ephedraceae, and Fabaceae
	3873	Cyperaceae, Compositae, Gramineae, Rosaceae, Ephedraceae, and Fabaceae
	3843	Cyperaceae, Gramineae, Tamaricaceae, and Polygonaceae
Jiangmanjiaer glacier foreland	4241	Gramineae and Compositae
	4206	Gramineae, Compositae, Fabaceae, and Caryophyllaceae
	4185	Gramineae, Compositae, Fabaceae, and Caryophyllaceae
	4149	Gramineae, Compositae, Fabaceae, Rosaceae, and Crassulaceae
	4063	Gramineae and Compositae
	4010	Gramineae and Compositae
	3793	Gramineae, Compositae, and Chenopodiaceae
	3730	Gramineae and Cyperaceae
	3661	Gramineae and Cyperaceae
	3631	Gramineae and Cyperaceae
Koxkar Baxi glacier foreland	3099	No
	3049	No
	3011	Rosaceae
	2992	Gramineae, Cyperaceae, Polygonaceae, Crassulaceae, and Asteraceae
	2988	Gramineae, Cyperaceae, Polygonaceae, Crassulaceae, and Asteraceae
	2986	Gramineae, Cyperaceae, Polygonaceae, Crassulaceae, and Asteraceae
	2979	Gramineae, Cyperaceae, Polygonaceae, Crassulaceae, and Asteraceae

2.5 Linear mixed-effects model

The linear mixed-effects model was applied to assess the changes in FVC as a function of GC (Meng et al., 2007). Fixed and random effects, as the major components of the model, had to be determined prior to calculation. Specifically, we first analyzed the effect of GC on FVC; therefore, GC could be considered as the fixed effect. At the glacier basin scale, aspect affected soil hydrothermal conditions via altering solar irradiation and subsequently altered the vegetation pattern. At the regional scale, the regional climate was one of the key elements influencing vegetation development. This led to the identification of regional climate and aspect as random effects. The analyses were conducted using the lme function in the nlme package in the statistical program R v. 3.6.1 (https://cran.r-project.org/). Finally, we used the r.squaredGLMM in the MuMIn package in the statistical program R v. 3.6.1 for the purpose of assessing the accuracy of the model. The function provided two measures: R^2m and R^2c. The first reports the R^2 of the model with just fixed effects, whereas the second represents the R^2 of the full model (including fixed and random effects). R^2 is the criteria indicating the fitness of the models. If R^2 is similar between models, it is most importantly that R^2c is only slightly different compared to R^2m, which implies that the inclusion of random effects does not improve the accuracy.

3 Results

3.1 FVC along elevational gradients

On the Jiangmanjiaer and Kekesayi glacier forelands of the eastern Pamir Plateau, FVC varied in an inverted "N-shaped" pattern with increasing elevation, but it exhibited declining trends with increasing elevation in general (Fig. 5). FVC was highest on the bottom of valleys (old sites), whereas it was lowest near the glacier terminus (young sites). Particularly, on the Jiangmanjiaer glacier foreland, the maximum and minimum of FVC were 91.9% (at 3631 m a.s.l.) and 4.8% (at

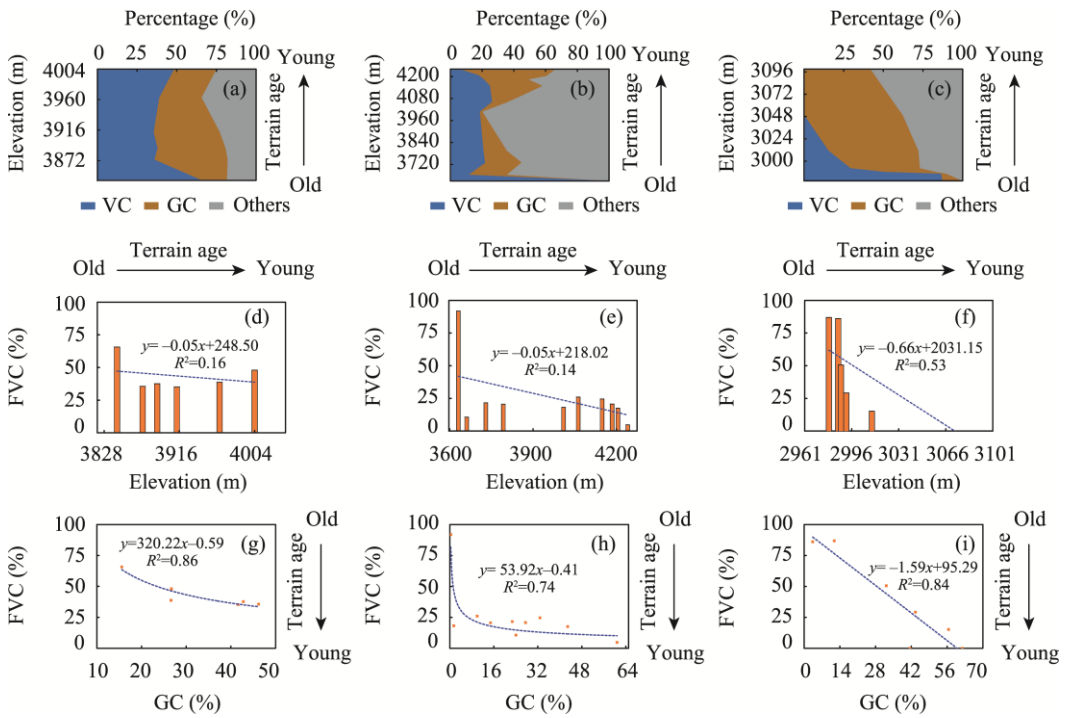

Fig. 5 Variations in percentages of land cover types (glacial gravel, vegetation, and others) along elevational gradients and the relationships between GC and FVC on the Kekesayi glacier foreland (a, d, and g), Jiangmanjiaer glacier foreland (b, e, and h), and Koxkar Baxi glacier foreland (c, f, and i). VC, vegetation cover.

4241 m a.s.l.), respectively, whereas those on the Kekesayi glacier foreland were 65.7% (at 3843 m a.s.l.) and 35.2% (at 3913 m a.s.l.), respectively. Furthermore, the spatial variation of FVC on the Jiangmanjiaer glacier foreland was more dramatic in contrast to that on the Kekesayi glacier foreland, with a range of 87.1%, while the Kekesayi glacier foreland was densely vegetated (Fig. 5).

On the Koxkar Baxi glacier foreland of the western Tianshan Mountains, FVC exhibited a linear decline trend with increasing elevation (Fig. 5c and f). Just like the spatial changes in FVC on the two glacier forelands of the eastern Pamir Plateau, its maximum (86.9%), as well as the minimum (0.0%), also occurred on the valley floor (old sites) and at the glacier terminus (young sites). FVC on the Koxkar Baxi glacier foreland of the western Tianshan Mountains showed a more pronounced growth trend with decreasing elevation compared with that on the two glacier forelands of the eastern Pamir Plateau (Fig. 5).

3.2 Plant family composition along elevational gradients

On the Kekesayi and Jiangmanjiaer glacier forelands, despite the fact that the surveyed glacier forelands were covered by cold-desert vegetation, the types and number of plant families displayed obvious differences along elevational gradients. On the Kekesayi glacier foreland, vegetation was primarily composed of individuals of the following families: Gramineae, Compositae, Cyperaceae, Ephedraceae, Fabaceae, Rosaceae, Tamaricaceae, and Polygonaceae. Cyperaceae was the dominant plant family and appeared at all sampling sites, whereas Tamaricaceae and Polygonaceae were the rarest plant families, only present near the bottom of valleys (old sites; Table 2). From the elevation of 4004 m a.s.l. to the glacier terminus (young sites), the land was covered by a lot of loose glacial gravel and sparse vegetation; thus, the simplest plant family composition appeared there. Moreover, the near valley bottom (3873 m a.s.l.) had the richest plant families, comprising 75.0% of all plant families. Plant family composition at the valley bottom (old sites) was simple and relatively stable; four plant families existed in this area, namely Gramineae, Cyperaceae, Tamaricaceae, and Polygonaceae. On the Jiangmanjiaer glacier foreland, the plant families consisted of Gramineae, Compositae, Cyperaceae, Fabaceae, Caryophyllaceae, Rosaceae, Crassulaceae, and Chenopodiaceae. Gramineae was the leading family and occurred at all sampling sites (Table 2). The variation in plant family composition along elevational gradients was stochastic. The richest plant family composition appeared at 4149 m a.s.l., whereas the simplest plant family composition occurred from the elevation of 4241 m a.s.l. to the glacier terminus (young sites). Even though each sampling site contained specific dominant species, *Artemisia minor* and *Carex moorcroftii* were the dominant species found at all sampling sites on the Kekesayi and Jiangmanjiaer glacier forelands, respectively (Fig. 6a and b).

On the Koxkar Baxi glacier foreland, overall six plant families were recorded, including Rosaceae, Gramineae, Cyperaceae, Polygonaceae, Crassulaceae, and Asteraceae. From the elevation of 3049 m a.s.l. to the glacier terminus (young sites), there was no vegetation on the barren land; however, there was plenty of glacial gravel. Plants did not appear until the elevation of 3011 m a.s.l., in which only plants of Rosaceous family were distributed sporadically in the surroundings of glacial gravel or in crevices among them (Fig. 2h). With lowering elevation, plant family composition became increasingly abundant. Finally, a stable alpine meadow appeared on the valley floor (2979 m a.s.l.), where plant family composition was the richest and consisted of Gramineae, Cyperaceae, Polygonaceae, Crassulaceae, and Asteraceae (Fig. 2i; Table 2). *Kobresia pygmaea* and *Carex melanantha* were widely distributed below 2992 m a.s.l. (Fig. 6c).

3.3 Species richness along elevational gradients

On the Kekesayi and Koxkar Baxi glacier forelands, species richness first increased and subsequently decreased with increasing elevation (Fig. 7). Their maximum and minimum occurred near the bottom of valleys (old sites) and near the glacier terminus (young sites), respectively. On the Jiangmanjiaer glacier foreland, species richness displayed a fluctuant change of decreasing firstly, then increasing, and finally decreasing with rising elevation. The sites where

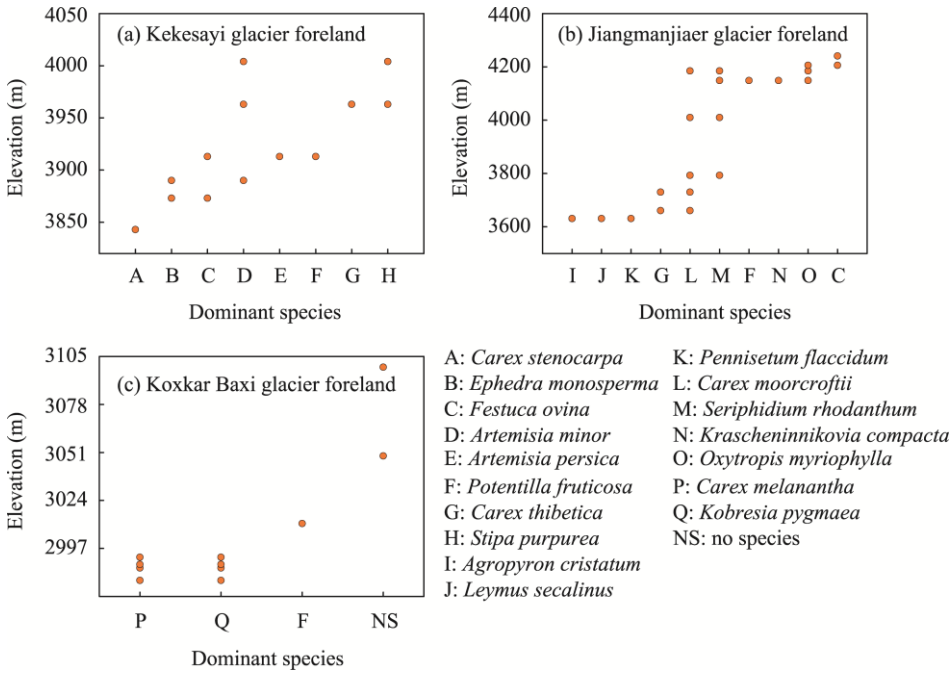

Fig. 6 Spatial distribution of the dominant species along elevational gradients on the Kekesayi glacier foreland (a), Jiangmanjiaer glacier foreland (b) and Koxkar Baxi glacier foreland (c)

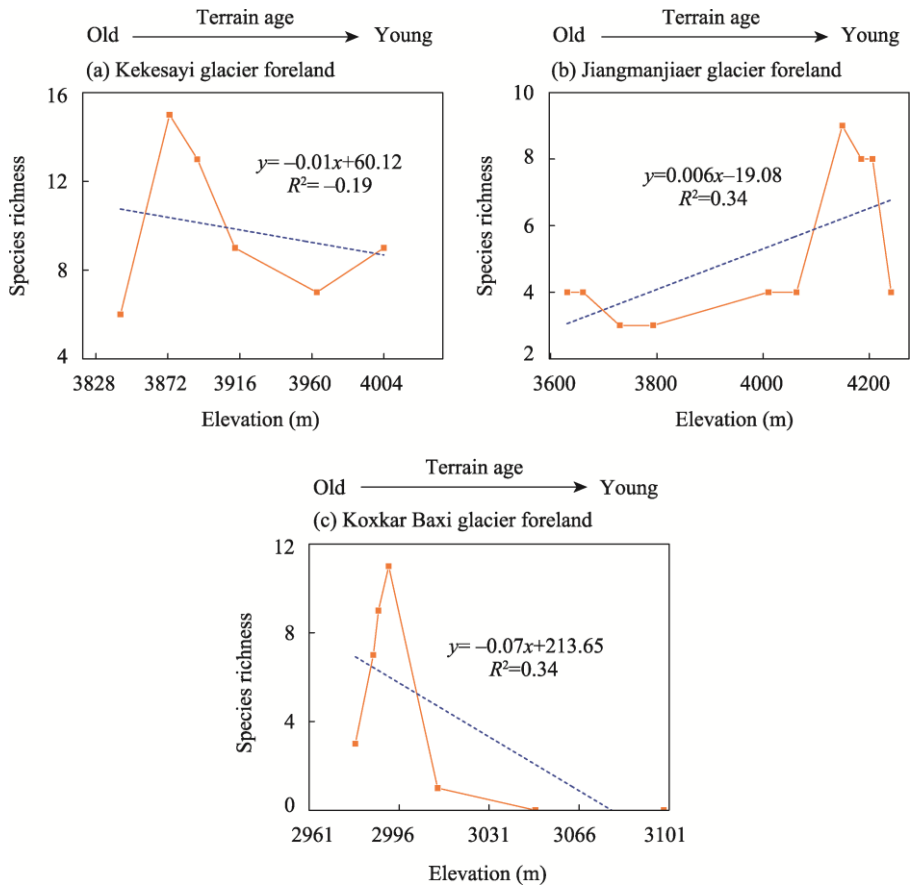

Fig. 7 Variations of species richness along elevational gradients on the Kekesayi glacier foreland (a), Jiangmanjiaer glacier foreland (b), and Koxkar Baxi glacier foreland (c)

the extremum occurred were totally opposite to those on the other glacier forelands (Fig. 7).

Overall, species richness exhibited decreasing trends on the Kekesayi and Koxkar Baxi glacier forelands with increasing elevation; however, it showed an increasing trend on the Jiangmanjiaer glacier foreland with rising elevation (Fig. 7).

4 Discussion

4.1 Community development of vascular plants on the three glacier forelands

In the early stage of plant community development, vascular plants on the all glacier forelands shared a similar picture of low FVC and species diversity (Burga et al., 2010; Schumann et al., 2016), whereas this landscape started to differ in the middle and later succession stages among the glacier forelands as a result of multiple factors, such as natural disturbances, terrain age, regional climate, topographic conditions, and so on (Tishkov, 1986; Jones and Roger, 2005; Raffl et al., 2006; Dolezal et al., 2008; Burga et al., 2010; Wietrzyk et al., 2018). As a matter of fact, this natural scene also occurred on the three surveyed glacier forelands. In the newly exposed surfaces after the glacier retreated, certain microorganisms first colonized on the barren land, and eventually their dead organic matter facilitated the colonization of pioneer plants by supplying the initial soil as well as nutrient conditions. Accordingly, the early stage of plant community development had the lowest FVC and species abundance, which was in accordance with earlier studies on the Urumqi Glacier No. 1 foreland of northwestern China (Wei et al., 2021), Skaftafellsjökull glacier foreland of southern Iceland (Glausen and Tanner, 2019), and glacier foreland in the European Alps (Schumann et al., 2016). These colonized pioneer plants further promoted the soil development and the accumulation of nutrients in soil (Wietrzyk et al., 2018), and thereafter vascular plants began to expand as succession proceeded. The spatial changes in vascular plant characteristics (FVC, plant family composition, and species diversity) had evident differences under different topographic (elevation and aspect) and climatic conditions. Specifically, despite the fact that FVC on the Kekesayi and Jiangmanjiaer glacier forelands located in the same glacier basin presented a similar variation trend along elevational gradients, the shady slope (Kekesayi) was more densely vegetated in contrast to the sunny slope (Jiangmanjiaer). Moreover, the Kekesayi glacier foreland had formed small vegetation patches, whereas vegetation on the Jiangmanjiaer glacier foreland tended to grow individually with the exception of the bottom of the valley where a grassland occurred. This was consistent with previous literature findings (Ostendorf and Reynolds, 1998; Pearson et al., 1999; Schumann et al., 2016). Furthermore, plant species diversity on the Kekesayi glacier foreland was more abundant compared with that on the Jiangmanjiaer glacier foreland. This pointed out the fact that change in solar radiation caused by aspect might accelerate heat and moisture migration of topsoil, and subsequently could alter the spatial pattern of vegetation colonization and development. Our results were consistent with previous studies (Ostendorf and Reynolds, 1998; Schumann et al., 2016), which indicated that aspect affects communities through altering solar insolation and hence temperature and effective moisture, thereby impacting biodiversity and composition.

In addition to topographic factors, regional climate was another critical factor affecting vegetation dynamics. However, its effect on vegetation had usually been neglected except for the studies of Robbins and Matthews (2010) and Schumann et al. (2016). Meteorological data (Table 1) revealed that climatic conditions on the survey glacier forelands of the eastern Pamir Plateau were colder and drier than those on the survey glacier foreland of the western Tianshan Mountains. Naturally, the difference in climatic conditions was also reflected in the ecosystem structure in the later stage of plant community development. In particular, on the relatively warm and humid glacier foreland (Koxkar Baxi), elevational zonality of vegetation was obvious, and an alpine meadow (at 2979 m a.s.l.) emerged just 576 m from the glacier terminus (Fig. 2i). On the other hand, the cold and dry glacier forelands of the eastern Pamir Plateau had sparse and scattered vascular plants and only progressed toward alpine grassland. This finding was consistent

with the study on the glacier forelands of the eastern and western Alps (Schumann et al., 2016). The study on the European Alps, nevertheless, contended that the differences in vegetation on the glacier forelands of the eastern and western Alps could not be explained by distinct climatic conditions, but rather by different species pools and treeline elevation (Schumann et al., 2016).

4.2 Effects of glacial gravel on plant colonization and development on the three glacier forelands

In the harsh environment of glacier forelands, vegetation colonization and development were primarily dominated by multiple biotic and abiotic factors, which made vegetation colonization in the early succession stage extremely difficult, and only a few pioneer plants had an opportunity to colonize in these barren lands (Dong et al., 2016). The three glacier forelands that were surveyed likewise experienced a similar situation. Interestingly, these pioneer species usually grew on the sides of glacial gravel or in the gaps, which was especially common on the newly exposed surfaces. Previous studies highlighted that this occurrence revealed how plants adapted to their harsh environment, but these studies only provided a qualitative account of how glacial gravel aided in the colonization and growth of vegetation (Thuiller et al., 2005; Mondoni et al., 2015).

In this study, we quantitatively explored the function of glacial gravel in the colonization and growth of vascular plants on the glacier forelands. In the entire stages of plant community development, FVC was negatively related to GC (Fig. 5g–i; Table 3), but their relationships varied depending on the different topographic and climatic conditions. Specifically, FVC on the glacier forelands of the eastern Pamir Plateau and western Tianshan Mountains decreased in a power function and a linear function with increasing GC, respectively. In addition to the spatial relationships between vascular plants and glacial gravel (Figs. 2a and b, and 5g and h), we speculated that glacial gravel might facilitate early stage vegetation colonization and development by providing suitable hydrothermal conditions and preventing damage of herbivores, but it might also impose potential restrictions on vegetation expansion in the middle and late stages by reducing available space. Similar findings from earlier investigations have been reported (Stöcklin and Bäumler, 1996; Jumpponen et al., 1999; Niederfriniger Schlag and Erschbamer, 2000; Mong and Vetaas, 2006). According to Table 3, R^2c was significantly different from R^2m when we analyzed the changes in FVC as a function of GC on the glacier forelands of the eastern Pamir Plateau, suggesting that aspect could improve the model accuracy. This finding indicated that the effect of aspect on vegetation should not be neglected when analyzing the role of glacial gravel in vegetation development at the basin scale. In addition, it has been found that R^2c was higher than R^2m when evaluating the changes in VC as a function of GC in the eastern Pamir Plateau and western Tianshan Mountains (Table 3), implying that the effect of glacial gravel on vegetation distribution was mediated by regional climate at the regional scale.

Table 3 Effects of gravel cover (GC) on fractional vegetation cover (FVC) at the glacier basin and regional scales using linear mixed-effects model and the assessment of the model accuracy

Response	Region	AIC	BIC	logLik	Intercept	Slope	R^2	R^2m	R^2c
Change in FVC as a function of GC	EP	144.15	147.98	–66.07	54.82	3.76*	–0.53	0.21	0.59
	EP-WT	212.45	218.72	–100.23	63.30	6.15*	–0.74	0.37	0.43

Note: EP represents the eastern Pamir Plateau; EP-WT represents the eastern Pamir Plateau and western Tianshan Mountains; AIC, BIC, and logLik are the Akaike, Schwarz-Bayesian Information Criterion, and logarithmic likelihood used for model selection, respectively; Intercept and Slope are the two parameters of the linear mixed-effects model; R^2 is the criteria indicating the fitness of the models; R^2m and R^2c are the two measures of the assessment of the model accuracy. *, P<0.05 level.

4.3 Advantages and limitations of UAV in the investigation of vegetation on the glacier forelands

The UAV has been extensively employed in studying vegetation dynamics in recent years (Dunford et al., 2009; Chen et al., 2016; Mead and Arthur, 2020). However, its application for the investigation of vegetation on the glacier forelands is rarely reported with the exceptions of Eichel

et al. (2017) and Wei et al. (2021). In this study, we investigated the vegetation data (FVC, plant family composition, and species richness) on the three glacier forelands using an UAV, which demonstrated five benefits that are mentioned in Section 1. However, this advanced approach also had its limitations, including species identification in the laboratory requiring lots of time, low quality of aerial photographs affecting the outcomes of species identification, and specific plants (creeping and low-growing plants, and plants that matched ground colors) increasing difficulties in FVC extraction and species identification (Wei et al., 2021). Furthermore, the inherent advantages of UAV in monitoring vegetation were further constrained by adverse field time, which was also evident in this study.

5 Conclusions

This study aimed at assessing the spatial differences of vascular plant community development on the three glacier forelands (Kekesayi, Jiangmanjiaer, and Koxkar Baxi) under various topographic and climatic conditions, as well as exploring the effects of glacial gravel on plant community development by integrating the ground-based sampling and aerial photography. The findings pointed out that the community characteristics of vascular plants exhibited different spatial changes along elevational gradients at different spatial scales. Specifically, at the glacier basin scale, the shady slope (Kekesayi) was more vegetated in comparison to the sunny slope (Jiangmanjiaer); at the regional scale, the relatively warm and humid glacier foreland (Koxkar Baxi) had the highest FVC. Meanwhile, species diversity of vascular plants on the glacier forelands gradually decreased as elevational gradients increased, with the exception of that on the Jiangmanjiaer glacier foreland. Moreover, the correlations between GC and FVC showed that the role of glacial gravel in the colonization and development of vascular plants varied as community succession proceeded. Namely, glacial gravel tended to play a positive role in plant colonization of the early stage; however, it played a negative role in the plant community development of the middle and later stages. Numerous other factors, such as topography (elevation and aspect) and climate, also had an impact on this phenomenon. These findings provided a strong implication for ecological restoration in glacier areas with harsh environment.

Acknowledgements

This research was supported by the Strategic Priority Research Program of Chinese Academy of Sciences (XDA19070501), the National Natural Science Foundation of China (41671066), the Ministry of Science and Technology of the People's Republic of China (2018FY100502), the Young Scholars Science Foundation of Lanzhou Jiaotong University (1200061124), and the International Partnership Program of Chinese Academy of Sciences (131C11KYSB20160061). The authors are grateful to Mr. LIU Jun and Mr. LI Da for their help with the fieldwork, Dr. YANG Shuping from Shihezi University, China for her guidance in dominant species identification, and Dr. YANG Junhua for the language editing of this manuscript.

References

Boulton G S. 1978. Boulder shapes and grain-size distributions of debris as indicators of transport paths through a glacier and till genesis. Sedimentology, 25(6): 773–799.

Burga C A, Krüsi B, Wernli M, et al. 2010. Plant succession and soil development on the foreland of the Morteratsch glacier (Pontresina, Switzerland): Straight forward or chaotic? Flora, 205(9): 561–576.

Chang L, He Y Q, Yang T B, et al. 2014. Analysis of herbaceous plant succession and dispersal mechanisms in deglaciated terrain on Mt. Yulong, China. The Scientific World Journal, 2014: 154539, doi: 10.1155/2014/154539.

Chen J J, Yi S H, Qin Y, et al. 2016. Improving estimates of fractional vegetation cover based on UAV in alpine grassland on the Qinghai–Tibetan Plateau. International Journal of Remote Sensing, 37(8): 1922–1936.

Cui Z J. 1960. Some characteristics of glaciers in the Muztag Ata-Kongur Tagh and their conditions for development and utilization. Acta Geographica Sinica, 26(1): 35–44. (in Chinese)

Dolezal J, Homma K, Takahashi K, et al. 2008. Primary succession following deglaciation at Koryto Glacier Valley, Kamchatka. Arctic, Antarctic, and Alpine Research, 40(2): 309–322.

Dong K, Tripathi B, Moroenyane I, et al. 2016. Soil fungal community development in a high Arctic glacier foreland follows a directional replacement model, with a mid-successional diversity maximum. Scientific Reports, 6: 26360, doi: 10.1038/srep26360.

Duan K Q, Yao T D, Wang N L, et al. 2007. Records of precipitation in the Muztag Ata Ice Core and its climate significance to glacier water resource. Journal of Glaciology and Geocryology, 29(5): 680–684. (in Chinese)

Dunford R, Michel K, Gagnage M, et al. 2009. Potential and constraints of Unmanned Aerial Vehicle technology for the characterization of Mediterranean riparian forest. International Journal of Remote Sensing, 30(19): 4915–4935.

Eichel J, Draebing D, Klingbeil L, et al. 2017. Solifluction meets vegetation: the role of biogeomorphic feedbacks for turf-banked solifluction lobe development. Earth Surface Processes & Landforms, 42(11): 1623–1635.

Glausen T G, Tanner L H. 2019. Successional trends and processes on a glacial foreland in Southern Iceland studied by repeated species counts. Ecological Processes, 8(1): 138–148.

Han H D, Liu S Y, Ding Y J, et al. 2008. Near-surface meteorological characteristics on the Koxkar Baxi Glacier, Tianshan. Journal of Glaciology and Geocryology, 30(6): 967–975. (in Chinese)

He L, Tang Y. 2008. Soil development along primary succession sequences on glacial gravels of Hailuogou Glacier, Gongga Mountain, Sichuan, China. CATENA, 72(2): 259–269.

He X B, Ding Y J, Liu S Y, et al. 2005. Obsevation and analyses of hydrological process of the Kaltamak Glacier in Muztag Ata. Journal of Glaciology and Geocryology, 27(2): 262–268. (in Chinese)

Holzer N, Vijay S, Yao T, et al. 2015. Four decades of glacier variations at Muztagh Ata (eastern Pamir): a multi-sensor study including Hexagon KH-9 and Pléiades data. The Cryosphere, 9(6): 2071–2088.

Houle G. 1997. No evidence for interspecific interactions between plants in the first stage of succession on coastal dunes in subarctic Quebec, Canada. Canadian Journal of Botany, 75(6): 902–915.

IPCC. 2012. Managing the Risks of Extreme Events and Disasters to Advance Climate Change Adaptation. In: Field C B, Barros V, Stocker T F, et al. Cambridge: Cambridge University Press, 1–582.

Jones C C, Roger D M. 2005. Patterns of primary succession on the foreland of Coleman Glacier, Washington, USA. Plant Ecology, 180(1): 105–116.

Jumpponen A, Väre H, Mattson K G, et al. 1999. Characterization of "safe sites" for pioneers in primary succession on recently deglaciated terrain. Journal of Ecology, 87(1): 98–105.

Leclercq P W, Oerlemans J, Cogley J G. 2011. Estimating the glacier contribution to sea-level rise for the Period 1800–2005. Surveys in Geophysics, 32: 519–535.

Lee T, Yeh H. 2009. Applying remote sensing techniques to monitor shifting wetland vegetation: A case study of Danshui River estuary mangrove communities, Taiwan. Ecological Engineering, 35(4): 487–496.

Li J, Liu S Y, Han H D, et al. 2012. Evaluation of runoff from Koxkar Glacier Basin, Tianshan Mountains, China. Climate Change Research, 8(5): 350–356. (in Chinese)

Li X, Xiong S F. 1995. Vegetation primary succession on glacier foreland in Hailuogou, MT. Gongga. Mountain Research, 12(2): 109–115. (in Chinese)

Li Y J, Ding Y J, Shangguan D H, et al. 2019. Regional differences in global glacier retreat from 1980 to 2015. Advances in Climate Change Research, 10(4): 203–213.

Li Z, Sun W X, Zeng Q Z. 1998. Measurements of glacier variation in the Tibetan Plateau using Landsat data. Remote Sensing of Environment, 63(3): 258–264.

Lillesand T M, Kiefer R W. 2000. Remote Sensing and Image Interpretation (4th ed.). New York: John Willy Sons Inc., 1–736.

Liu S Y, Sun W X, Shen Y P, et al. 2003. Glacier changes since the Little Ice Age maximum in the western Qilian Shan, northwest China, and consequences of glacier runoff for water supply. Journal of Glaciology, 49(164): 117–124.

Liu S Y, Yao X J, Guo W Q, et al. 2015. The contemporary glaciers in China based on the Second Chinese Glacier Inventory. Acta Geographica Sinica, 70(1): 3–16. (in Chinese)

Luo Z Q. 1994. Preliminary study on the hydrological characteristics and calculation of the Gaizi River in Xinjiang. Hunan Water Conservancy, (6): 17–19. (in Chinese)

Martínez-López J, Carreño M F, Palazón-Ferrando J A, et al. 2014. Remote sensing of plant communities as a tool for assessing the condition of semiarid Mediterranean saline wetlands in agricultural catchments. International Journal of Applied Earth Observation and Geoinformation, 26(1): 193–204.

Mead L, Arthur M. 2020. Environmental condition in British moorlands: quantifying the life cycle of *Calluna vulgaris* using UAV aerial imagery. International Journal of Remote Sensing, 41(2): 573–583.

Meng Q M, Cieszewski C J, Madden M, et al. 2007. A linear mixed-effects model of biomass and volume of trees using Landsat ETM+ images. Forest Ecology and Management, 244(1–3): 93–101.

Mondoni A, Pedrini S, Bernareggi G, et al. 2015. Climate warming could increase recruitment success in glacier foreland plants. Annals of Botany, 116(6): 907–916.

Mong C E, Vetaas O R. 2006. Establishment of *Pinus wallichiana* on a Himalayan glacier foreland: Stochastic distribution or safe sites? Arctic, Antarctic, and Alpine Research, 38(4): 584–592.

Muzein B S. 2006. Remote sensing and GIS for land cover/land use change detection and analysis in the semi-natural

ecosystems and agriculture landscapes of the Central Ethiopian Rift Valley. PhD Dissertation. Dresden: Techniche Universität Dresden.

Niederfriniger Schlag R, Erschbamer B. 2000. Germination and establishment of seedlings on a glacier foreland in the central Alps, Austria. Arctic, Antarctic, and Alpine Research, 32(3): 270–277.

Ostendorf B, Reynolds J F. 1998. A model of arctic tundra vegetation derived from topographic gradients. Landscape Ecology, 13(3): 187–201.

Pearson S M, Turner M G, Drake J B. 1999. Landscape change and habitat availability in the Southern Appalachian Highlands and Olympic Peninsula. Ecological Application, 9(4): 1288–1304.

Raffl C, Mallaun M, Mayer R, et al. 2006. Vegetation succession pattern and diversity changes in a Glacier Valley, Central Alps, Austria. Arctic, Antarctic, and Alpine Research, 38(3): 421–428.

RGI Consortium. 2017. Randolph Glacier Inventory - A Dataset of Global Glacier Outlines, Version 6. Boulder, Colorado USA. National Snow and Ice Data Center. [2021-07-20]. https://doi.org/10.7265/4m1f-gd79.

Robbins J A, Matthews J A. 2010. Regional variation in successional trajectories and rates of vegetation change on glacier forelands in south-central Norway. Arctic, Antarctic, and Alpine Research, 42(3): 351–361.

Rooney T P. 1997. Escaping herbivory: Refuge effects on the morphology and shoot demography of the clonal forest herb *Maianthemum canadense*. Journal of the Torrey Botanical Society, 124(4): 280–285.

Sabit M, Mamat Y, Nasirdin N. 2016. Landscape characteristics of the vertical natural zones of Tianshan Tomur Nature Reserve. Journal of Glaciology and Geocryology, 38(5): 1425–1431. (in Chinese)

Schumann K, Gewolf S, Tackenberg O. 2016. Factors affecting primary succession of glacier foreland vegetation in the European Alps. Alpine Botany, 126(2): 105–117.

Seong Y B, Owen L A, Yi C L, et al. 2009a. Quaternary glaciation of Muztag Ata and Kongur Shan: Evidence for glacier response to rapid climate changes throughout the late glacial and holocene in westernmost Tibet. Bulletin of the Geological Society of America, 121(3–4): 348–365.

Seong Y B, Owen L A, Yi C L, et al. 2009b. Geomorphology of anomalously high glaciated mountains at the northwestern end of Tibet: Muztag Ata and Kongur Shan. Geomorphology, 103(2): 227–250.

Shangguan D H, Liu S Y, Ding Y J, et al. 2006. Monitoring the glacier changes in the Muztag Ata and Konggur mountains, east Pamirs, based on Chinese Glacier Inventory and recent satellite imagery. Annals of Glaciology, 43(1): 79–85.

Stöcklin J, Bäumler E. 1996. Seed rain, seedling establishment and clonal growth strategies on a glacier foreland. Journal of Vegetation Science, 7(1): 45–56.

Sun Y, Yi S H, Hou F J. 2018. Unmanned aerial vehicle methods makes species composition monitoring easier in grasslands. Ecological Indicator, 95: 825–830.

Thuiller W, Lavorel S, Araújo M B, et al. 2005. Climate change threats to plant diversity in Europe. Proceedings of the National Academy of Sciences of the United States of America, 102(23): 8245–8250.

Tishkov A A. 1986. Primary succession in arctic tundra on the west coast of Spitsbergen (Svalbard). Polar Geography and Geology, 10(2): 148–156.

Wang J, Zhou S Z, Zhao J D, et al. 2011. Quaternary glacial geomorphology and glaciations of Kongur Mountain, eastern Pamir, China. Science China Earth Sciences, 54(4): 591–602.

Wang Y T, Dai Z G, Yang S J, et al. 2016. The distribution of marco polo sheep and their habitat vegetation dynamics in east pamir. Acta Ecologica Sinica, 36(1): 209–217. (in Chinese)

Wei T F, Shangguan D H, Yi S H, et al. 2021. Characteristics and controls of vegetation and diversity changes monitored with an unmanned aerial vehicle (UAV) in the foreland of the Urumqi Glacier No. 1, Tianshan, China. Science of the Total Environment, 771(1): 145433, doi: 10.1016/j.scitotenv.2021.145433.

Wietrzyk P, Rola K, Osyczka P, et al. 2018. The relationships between soil chemical properties and vegetation succession in the aspect of changes of distance from the glacier forehead and time elapsed after glacier retreat in the Irenebreen foreland (NW Svalbard). Plant and Soil, 428(1–2): 195–211.

Xie C W, Ding Y J, Chen C P, et al. 2007. Study on the change of Keqikaer Glacier during the last 30 years, Mt. Tuomuer, Western China. Environmental Geology, 51(7): 1165–1170.

Yan S Y, Guo H D, Liu G, et al. 2013. Mountain glacier displacement estimation using a DEM-assisted offset tracking method with ALOS/PALSAR data. Remote Sensing Letters, 4(5): 494–503.

Yang H N, Yan S Y, Liu G, et al. 2014. Fluctuations and movements of the Kuksai Glacier, western China, derived from Landsat image sequences. Journal of Applied Remote Sensing, 8(1): 084599, doi: 10.1117/1.JRS.8.084599.

Yu W S, Yao T D, Tian L D, et al. 2006. Relationships between $\delta^{18}O$ in summer precipitation and temperature and moisture trajectories at Muztagata, western China. Science in China: Series D Earth Sciences, 49(1): 27–35.

Zhang Y, Liu S Y, Ding Y J. 2007. Glacier meltwater and runoff modelling, Keqicar Baqi Glacier, southwestern Tien Shan, China. Journal of Glaciology, 53(180): 91–98.

Zhang Z, Liu S Y, Wei J F, et al. 2016. Mass change of glaciers in Muztag Ata-Kongur Tagh, Eastern Pamir, China from 1971/76 to 2013/14 as derived from remote sensing data. PLoS ONE, 11(1): e0147327, doi: 10.1371/journal.pone.0147327.